Surface Modification of Polyurethane by Plasma-Induced Graft Polymerization of Poly(ethylene glycol) Methacrylate*

Y. X. QIU,[1,2,†] D. KLEE,[1] W. PLÜSTER,[1] B. SEVERICH,[1] and H. HÖCKER[1]

[1]Department of Textile and Macromolecular Chemistry, Aachen University of Technology, Veltmanplatz 8, 52062, Aachen, Germany; and [2]Department of Polymer Science and Engineering, Zhejiang University, Hangzhou, 310027, China

SYNOPSIS

A new approach, plasma-induced graft polymerization of poly(ethylene glycol) methacrylate (PEGMA), was used to introduce PEG graft chains with hydroxyl end groups onto a polyurethane (Tecoflex) surface. After argon plasma treatment and subsequent exposure to air, graft polymerization onto Tecoflex films was allowed to proceed in deaerated aqueous solutions of PEGMA at 60°C. The virgin, plasma-treated, and grafted films were characterized comparatively by means of attenuated total reflection infrared spectroscopy, X-ray photoelectron spectroscopy, atomic force microscopy, measurement of contact angle, and protein adsorption. The Tecoflex film undergoes etching during argon plasma treatment, surface oxidation when exposed to air after plasma treatment, and surface restructuring in response to environment upon storage in air. The plasma-induced graft polymerization of PEGMA proved to be successful in introducing PEG graft chains with reactive hydroxyl end groups onto the surface. Grafted films with different surface grafting density of PEG were prepared. Grafted films with higher PEG content exhibit higher hydrophilicity, smoother topography, and lower fibrinogen adsorption. The hydroxyl end groups built onto the surface offer further possibilities of improving its biocompatibility by immobilizing bioactive molecules.

INTRODUCTION

Polyurethanes (PUs) are extensively used for biomedical applications because of their excellent mechanical properties and comparatively good tissue and blood compatibility.[1] Grafting of poly(ethylene glycol) (PEG) onto the surface of PUs has frequently been used to improve the blood compatibility of polyurethanes.[2-9] It is accepted that the PEG chains presented at the PU surface result in reduced levels of protein adsorption and decreased platelet adhesion because of an excluded volume effect and dynamic motion of the water soluble PEG chains grafted onto the surface.[2]

The most commonly used method of introducing PEG chains onto the surfaces of PUs is a typical two-step procedure[3-9]: the PU surface was first treated with a diisocyanate, usually hexamethylene diisocyanate, to introduce free isocyanate groups, followed by coupling PEG using the reaction between the terminal isocyanate groups and the hydroxyl groups of PEG. The hydroxyl groups of PEG were further used to immobilize bioactive molecules such as heparin[3-9] or to create a heparin-like surface with negative charges by sulfonating with propane sultone.[10,11]

The gas plasma (or glow discharge) treatment technique has been widely used in surface modification of polymer materials because of the advantage that the modification is limited specifically to the surface region of the materials.[12,13] Ikada and coworkers[14] reported the graft polymerization of methoxy PEG methacrylate ($CH_2=C(CH_3)-CO-(OCH_2CH_2)_n-OCH_3$) onto a PU film by plasma discharge technique. The modified PU surface showed reduced protein adsorption and reduced platelet adhesion. However, the grafted PU surface is not accessible to further modification because the grafted PEG chains have nonreactive methoxy

* Presented at the 12th European Conference on Biomaterials, Porto, Portugal, Oct. 10–13, 1995.

† To whom correspondence should be addressed.

Journal of Applied Polymer Science, Vol. 61, 2373–2382 (1996)
 CCC 0021-8995/96/132373-10

Table I Chemical Composition and Structure of Tecoflex 60G

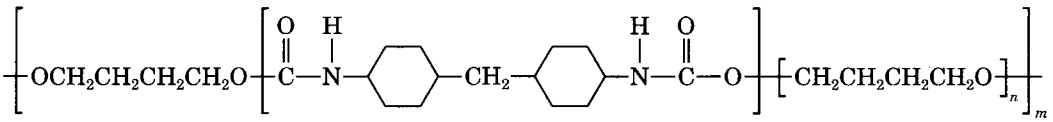

Constituent	Component	Molecular Weight	Content (wt %)
Polyether	Poly(tetramethylene glycol) (PTMG)	1000	46
Diisocyanate	Methylene bis(cyclohexyl) diisocyanate	262	42
Chain extender	1,4-Butanediol	90	12

($-OCH_3$) end groups. Sun et al.[15,16] studied the graft polymerization of the same monomer onto Silastic surface but using the radiation grafting technique. In the present study, plasma-induced graft polymerization of PEG methacrylate (PEGMA, $CH_2=C(CH_3)-CO-(OCH_2CH_2)_n-OH$) was used to introduce PEG graft chains with hydroxyl end groups onto the Tecoflex surface. Subsequently, heparin was immobilized via the hydroxyl end groups onto the Tecoflex surface.

EXPERIMENTAL

Materials

The PU used, Tecoflex 60G, is commercially available and was provided by Thermedics Inc. (Woburn, MA, USA). The chemical components and chemical structure of Tecoflex 60G are given in Table I. Granules of Tecoflex 60G were dissolved in tetrahydrofuran to a 10% (w/w) solution. This solution was casted on a melamine resin plate, and the solvent was allowed to evaporate at room temperature for more than 3 days. After Soxhlet extraction with an ethanol/hexane (21/79, w/w) mixture overnight, followed by vacuum drying overnight at 60°C, films with a thickness of about 0.4 mm were obtained. PEGMA ($CH_2=C(CH_3)-CO-(OCH_2CH_2)_n-OH$, n = 5, Aldrich) was purified by washing PEGMA-chloroform solution with saturated aqueous solution of sodium chloride and double-distilled water to remove the inhibitor hydroquinone monomethyl ether and recovered by evaporation of chloroform.

Plasma-Induced Graft Polymerization

Tecoflex films were treated with an argon plasma using a microwave plasma generator (a Hexagon Plasma Unit of Technics Plasma GmbH, Kirchheim,

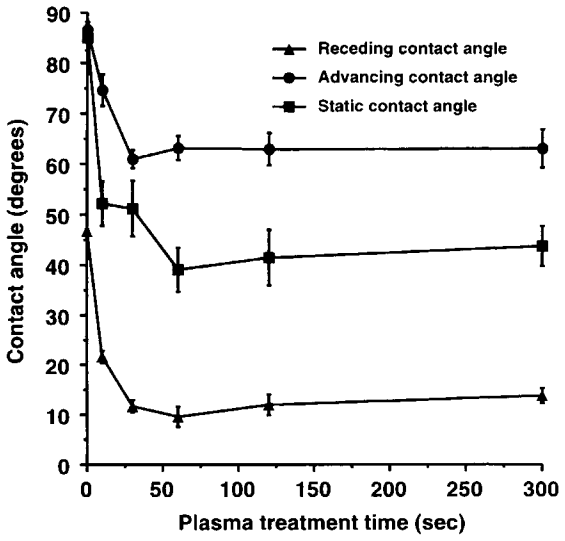

Figure 1 Dependence of contact angle on plasma treatment time. The static angles were measured by sessile drop method.

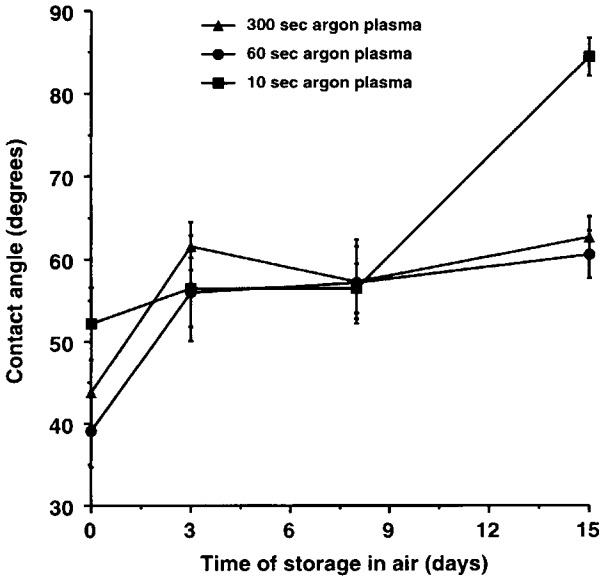

Figure 2 Change of the static contact angle on storage of the plasma-treated films in air.

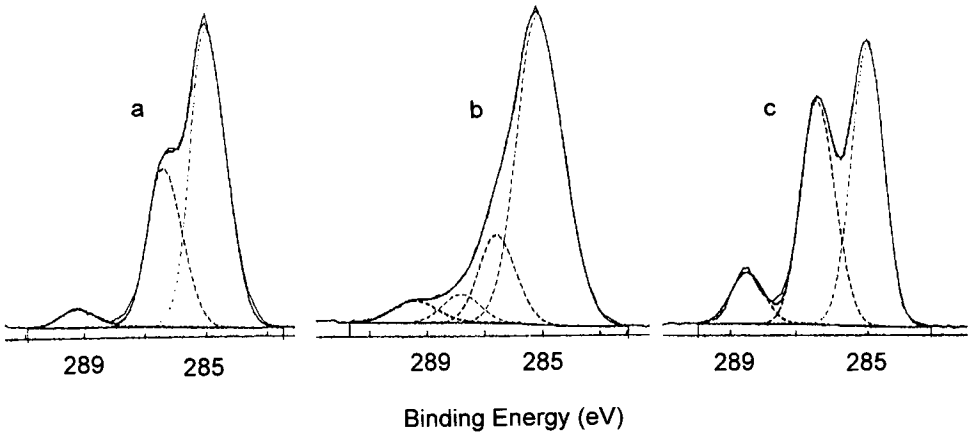

Figure 3 High-resolution C_{1S} XPS peaks of the virgin (a), plasma-treated (b), and PEG grafted (c) films.

Germany) with a frequency of 2.45 GHz, a plasma power of 300 W, and a gas flow rate of 16.8 mL/min at a pressure of 0.14 mbar. The films exposed to air less than 10 min after plasma treatment was immersed into degassed aqueous solutions of PEGMA (10% w/w) and kept at 60°C under magnetic stirring for a given time to allow the plasma-induced graft polymerization (PIGP) of PEGMA. The excessive PEGMA monomer and possible oligomer of PEGMA were removed from the grafted films by washing with water at room temperature overnight under vigorous stirring, followed by washing with ethanol in an ultrasonic water bath three times, each time for 10 min. The purified films were dried under vacuum overnight at 60°C.

Characterization of the Virgin, Plasma-Treated, and Grafted Films

Attenuated Total Reflection-IR (ATR-IR)

ATR-IR analyses were carried out on a Nicolet 60 SXR IR spectrometer. The spectra were recorded at an incident angle of 45 deg, using a germanium crystal as an internal-reflection element.

X-Ray Photoelectron Spectroscopy (XPS)

XPS spectra were recorded with an X-Probe 206 spectrometer (Surface Science Instruments, Mountain View, CA) with Al-K_α (1486.6 eV) as X-ray excitation source. Binding energies were referenced to the saturated hydrocarbon peak at 285.0 eV. The emission angle of electrons was set at 45 deg.

Atomic Force Microscopy (AFM)

A Digital Instruments Nanoscope III atomic force microscope was used to examine the surface topographical nature of the virgin, plasma-treated, and grafted films. The AFM images were acquired in ambient condition using the tapping mode.

Contact Angle Measurement

Static contact angles were measured using the sessile drop method or the water–air captive bubble method, using a contact angle meter G-23 (Krüss GmbH, Hamburg, Germany). The water drops were monitored by means of a video camera and the contact angle was evaluated from computer printouts of the video screen and expressed as an average value of six measurements. Dynamic contact angles were measured using the Wilhelmy plate technique in a KW-2P contact angle apparatus (H. Lemke & Partner Company, Kaarst, Germany). Four cycles for each sample with a speed of 10 mm/min were used in the measurement. The water used in the contact angle measurement was double-distilled water.

Protein Adsorption

All films were hydrated for 2 days before protein adsorption measurement. The adsorption of fibrinogen was measured semiquantitatively by an indirect enzyme-linked immunosorbent assay (ELISA). The adsorption of fibrinogen on the film surface was allowed at room temperature for 1 h. After removing the excessive fibrinogen, the adsorbed fibrinogen was specifically bound to a primary antibody [goat immunoglobulin-G 2a (IgG 2a)] and a peroxidase-labeled secondary antibody (horseradish peroxidase-goat IgG 3 conjugate) and thus forms a complex of antigen–antibody–antibody–peroxidase. The above complex was incubated with an H_2O_2-ABTS (hydrogen peroxide-[2,2′-azino-bis(3-ethylbenziothiazoline-6-

Table II Fraction of Carbon Functional Groups Derived From the High-Resolution C_{1S} XPS Peaks

		C_{1S} Peaks and Their Percentage			
Sample	Plasma Treatment Time (s)	C—H, C—C (285.0 eV)	C—O (286.5 eV)	—C=O (288.0 eV)	O ‖ N—C—O[a] (298.4 eV)
Virgin film	0	64.5	31.9	—	3.6
Plasma-treated films	10	56.9 (69.7)	32.4 (22.6)	3.9 (3.4)	6.8 (4.3)
	60	58.8 (65.4)	25.0 (22.1)	7.4 (5.2)	8.9 (7.3)
	120	62.0 (68.0)	23.1 (19.4)	7.3 (5.9)	7.3 (6.7)
	300	62.5 (73.0)	23.3 (16.6)	6.3 (5.4)	7.8 (5.0)

Data without parentheses are for samples exposed to air for a short time after plasma treatment and measured immediately. Data in parentheses are for samples stored in air after plasma treatment and measured about 3 days later.

[a] O ‖ N—C—O for the virgin film, O ‖ N—C—O and —O—C=O for the plasma treated films.

sulfonic acid) diammonium salt]) solution. H_2O_2 forms a stable complex with peroxidase. However, in the presence of an electron donor, for example, ABTS, the complex dissociates, reducing the enzyme back to its original state and releasing the oxidized electron donor which changes color. In this case, a metastable green intermediate of ABTS is formed and its concentration was measured by a microtiter plate reader (Spectra 2000, SLT-Lab Instruments) at 410 nm.

Immobilization of Heparin

The hydroxyl end groups of the grated films were activated with tosyl chloride.[17,18] The reference and activated films were immersed in buffer solutions containing 10 mg sodium salt of heparin (from porcine intestinal mucosa, Fluka). The immobilization reactions were allowed to continue under gentle stirring at 4°C for 24 h. The films were washed with phosphate-buffered solution overnight (4°C) and then briefly rinsed with water. The amount of immobilized heparin was measured using the toluidine blue (Sigma) method.[19]

RESULTS AND DISCUSSION

Effect of Plasma Treatment

Contact Angle Change

Both static and dynamic contact angles decrease obviously after a 10-s plasma treatment and then grad-

Table III Surface Elemental Composition of the Virgin Film, Plasma-Treated, and Grafted Films

Sample Type	Plasma Treatment Time (s)	Grafting Density ($\mu g/cm^2$)	C (mol %)	O (mol %)	N (mol %)	O/C (surface molar ratio)
Virgin film	0	/	78.71	18.28	3.02	0.232
Plasma-treated films	10	/	72.96 (77.21)	23.58 (18.96)	3.46 (3.50)	0.323 (0.246)
	60	/	72.65 (75.98)	22.43 (19.16)	4.92 (4.86)	0.309 (0.252)
	120	/	71.98 (76.33)	23.29 (19.30)	4.73 (4.37)	0.324 (0.253)
	300	/	67.70 (74.25)	26.26 (19.24)	6.04 (6.51)	0.388 (0.259)
Grafted films	10	91	73.76	25.35	0.98	0.344
	30	173	72.34	26.61	1.05	0.368
	300	341	72.14	27.17	0.51	0.377
	300	517	72.41	27.59	0.00	0.381
PEGMA	/	/	74.44	25.46	0.00	0.342

Data without parentheses are for samples exposed to air for a short time after plasma treatment and measured immediately. Data in parentheses are for sample stored in air after plasma treatment and measured about 3 days later.

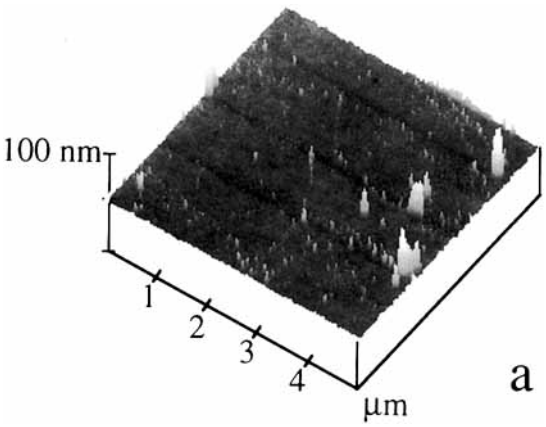

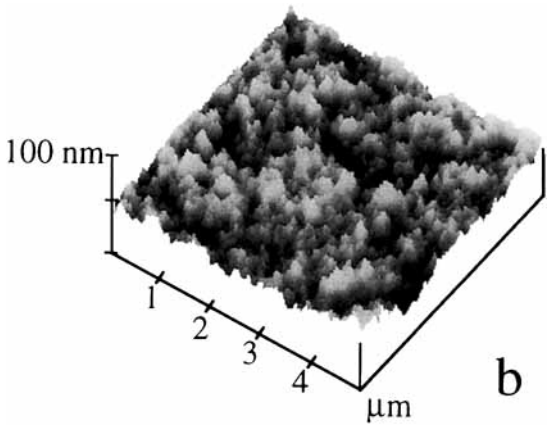

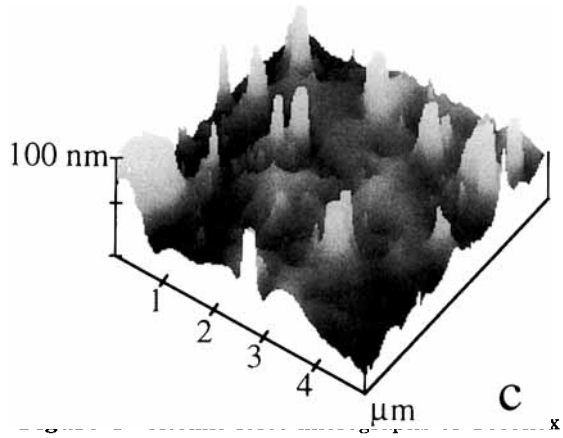

x films: (a) virgin (SMR = 0.9 nm), (b) 10-s argon plasma-treated (SMR = 4 nm), and (c) 300-s argon plasma-treated (SMR = 11 nm). The surface mean roughness (SMR) values were evaluated from corresponding micrographs with a surface area of 5 × 5 μm.

ually lower to a limiting value as the plasma treatment time is prolonged (Fig. 1). This is consistent with the well-accepted fact that polymer surfaces will exhibit higher hydrophilicity because of the introduction of polar groups from oxidation when exposed to air after inert gas plasma treatment, and the extent of oxidation greatly depends on the substrate material, the conditions of plasma treatment, and the design of the plasma reactor. However, upon storage in air, the low contact angles achieved by plasma treatment increase (Fig. 2). This indicates that the hydrophilicity of the plasma-treated Tecoflex surface decreases as a function of storage time because of surface restructuring in response to the hydrophobic air environment. This has been referred to as an aging phenomenon of plasma-treated polymer surfaces[13] or as hydrophobic recovery phenomenon of plasma treated polymer surfaces in air.[20-22]

XPS Results

In addition to the three C_{1S} peaks of the virgin film at 285.0, 286.5, and 289.4 eV [Fig. 3(a)], the plasma-treated film exhibits a C_{1S} peak at 288 eV [Fig. 3(b)]. This is ascribed to the newly formed —C=O groups arising from surface oxidation when Tecoflex film was exposed to air after argon plasma treatment.

The fractions of carbon functional groups derived from the high-resolution C_{1S} XPS peaks are shown in Table II. The data without brackets reflect the distribution of carbon functional groups for films right after plasma treatment. More than 3 mol % of newly formed —C=O groups was detected for the plasma-treated films. As compared with the virgin film, the plasma-treated films exhibit a lower percentage of C_{1S} peak at 285.0 eV and a higher percentage of C_{1S} peak at 289.4 eV. These results indicate clearly the oxidation of Tecoflex films that were exposed to air after argon plasma treatment. At the same time, however, a much lower mole percentage of C—O linkages (less than 25%, except for the 10-s plasma-treated film) on the plasma-treated surfaces as compared with the virgin surface (about 32%) was observed. During plasma treatment of a polymer surface, etching effect is always observed. In the case of Tecoflex surface, the PTMG soft segment is less polar than the methylene bis(cyclohexyl)diisocyanate hard segment and tends to accumulate at the polymer–air interface.[23] Hence, the PTMG domain is primarily susceptible to etching by the argon plasma, which results in a decrease of C—O linkages on the surface.

The differences between the data with and without brackets in Table II reflect the change in the distribution of carbon functional groups upon storage in air. The increase in the fraction of nonpolar component (C—H and C—C) and the decrease in the fraction of polar components (C—O, —C=O, —O—C=O, and $\begin{matrix} & O & \\ & \| & \\ N-C-O & & \end{matrix}$) upon storage in air

Table IV Fibrinogen Adsorption on the Surfaces of the Virgin Film, Plasma-treated, and Grafted Tecoflex Films Measured With an ELISA

Sample	Plasma Treatment Time (s)	Grafting Density (μg PEG/cm^2)	Contact Angle[a]	OD Value	Relative Adsorption (%)
Virgin film	0	/	58 ± 2.5	0.6695	100
Plasma-treated films	10	/	37 ± 2.8	0.2065	30.8
	60	/	34 ± 2.7	0.5885	87.9
	300	/	38 ± 3.0	0.6610	98.7
Grafted films	/	247	42 ± 3.6	0.5165	77.1
	/	280	40 ± 2.2	0.2010	30.0
	/	324	36 ± 1.8	0.1515	22.6
	/	420	35 ± 0.9	0.1255	18.7

[a] Static contact angle measured by captive bubble (air in water) method.

demonstrates the above mentioned hydrophobic recovery phenomenon.

Surface elemental composition of the virgin and the plasma-treated films provide further evidence for the existence of surface oxidation (Table III). Obviously higher surface oxygen contents and lower surface carbon contents were observed for the plasma-treated films as compared with the virgin film. The increase in the surface carbon content and the decrease in the surface oxygen content upon storage in air for the plasma-treated films corroborates the hydrophobic recovery phenomenon. It should be pointed out that nitrogen is also introduced to the surface region of the films when treated with argon plasma and subsequently exposed to air, a phenomenon not well-understood so far but also observed by other researchers.[24,25]

Surface Topography

The virgin film has a relatively smooth surface [Fig. 4(a), SMR = 0.9]; in contrast, plasma-treated films have rough surfaces on the scale of between nanometer to micrometer. If we take the value of surface mean roughness (SMR), the mean value of the surface relative to the center plane, as a quantitative measure, the 300-s plasma-treated film (SMR = 11), [Fig. 4(c)] has a much rougher surface than the 10-s plasma-treated film (SMR = 4) [Fig. 4(b)]. The increase in surface roughness caused by plasma treatment demonstrates the existence of the surface etching process.

Protein Adsorption

Usually, less protein adsorption will be observed on a more hydrophilic and/or smoother surface. This is also the case for plasma-treated Tecoflex films. A short time of plasma treatment of a Tecoflex film leads to a significant reduction of fibrinogen adsorption (Table IV). Only about 30.8% of fibrinogen adsorption was observed on the 10-s plasma-treated film with respect to that on the virgin film. The reason may be that the different hydrophilicity of these two films plays a major role in determining the protein adsorption behavior, despite the increase in surface roughness of the 10-s plasma-treated film. As the plasma treatment time was prolonged to 60 and 300 s; however, the fibrinogen adsorption increases to 87.9 and 98.7%, respectively. This is probably caused by the increase in surface roughness

Table V Effect of Plasma Treatment Time on the Graft Copolymerization

	Plasma Treatment Time (s)				
	10	30	60	120	300
Grafting density (μg PEG/cm^2)[a]	91	155	182	321	341
Grafting density (μg PEG/cm^2)[b]	97 ± 10 (n = 4)	164 ± 9 (n = 2)	181 ± 41 (n = 4)	373 ± 5 2 (n = 2)	382 ± 32 (n = 4)

[a] Data obtained from one batch of experiments.
[b] Average data from different batches of experiments. n is the number of repeated experiments.

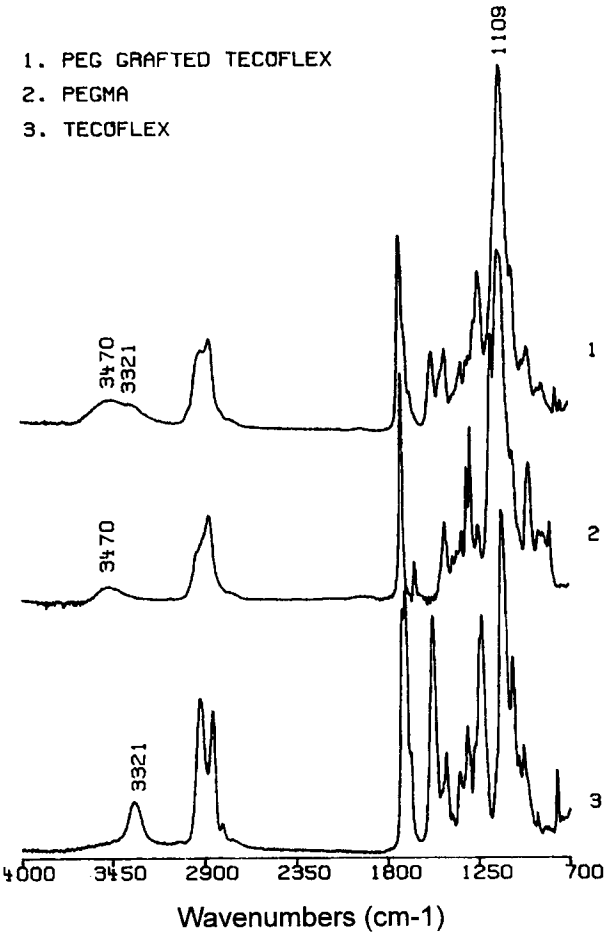

Figure 5 ATR-IR spectra of PEGMA, virgin, and PEG grafted Tecoflex film.

induced by the etching process from longer times of plasma treatment.

Plasma-Induced Graft Polymerization

Graft Polymerization

The graft copolymerization of PEGMA onto the argon plasma-treated Tecoflex films was carried out in an aqueous solution of PEGMA at 60°C for 5 h. The apparent increase in weight of the purified grafted films as compared with that of the virgin films can be regarded as a primary evidence for the occurring of graft copolymerization (Table V). Increasing in the grafting density with the plasma treatment time was observed. This trend is similar to some UV irradiation grafting systems[26-28] and an ozone-induced grafting system.[29] This has also been observed in the PIGP of acrylic acid onto polyamide.[27]

ATR-IR

PEG chains were successfully grafted onto the surface of Tecoflex films as indicated qualitatively by the IR spectra in Figure 5. In addition to the IR absorption bands of the virgin Tecoflex, a broad band centered around 3470 cm^{-1} corresponding to the presence of free hydroxyl groups was observed for the grafted films.

XPS Results

As expected, no new peaks were observed for the grafted films [Fig. 4(c)], but the qualitative trend of the C_{1S} peak (Table VI) and the data of composition (Table III) demonstrate the grafting of PEG onto the Tecoflex films. The fraction of C_{1S} peak of C—O at 286.5 eV increases systematically with the increase of surface PEG grafting density and simultaneously the fraction of C_{1S} peak of C—H and C—C at 285.0 eV decreases systematically, indicating clearly the appearance of PEG chains on the Tecoflex surface.

Furthermore, quantitative data of elemental composition (Table III) also demonstrated the success of PEG grafting onto the Tecoflex surface. An increase in the surface oxygen content and, at the same time, a decrease in the surface nitrogen content was observed for the grafted films. It is interesting

Table VI Fraction of Carbon Functional Groups Derived From High-Resolution C_{1S} XPS Peaks

			C_{1S} Peaks and Their Percentage		
Sample	Plasma Treatment Time (s)	Grafting Density (μg PEG/cm^2)	C—H, C—C (285.0 eV)	C—O (286.5 eV)	—(O)—C(=O)—(N) (~ 289 eV)
Virgin film	0	/	64.5	31.9	3.6
Grafted films	10	91	70.0	22.2	8.0
	30	173	60.2	29.8	10.0
	300	341	55.5	35.1	9.4
	300	517	51.5	38.5	10.0

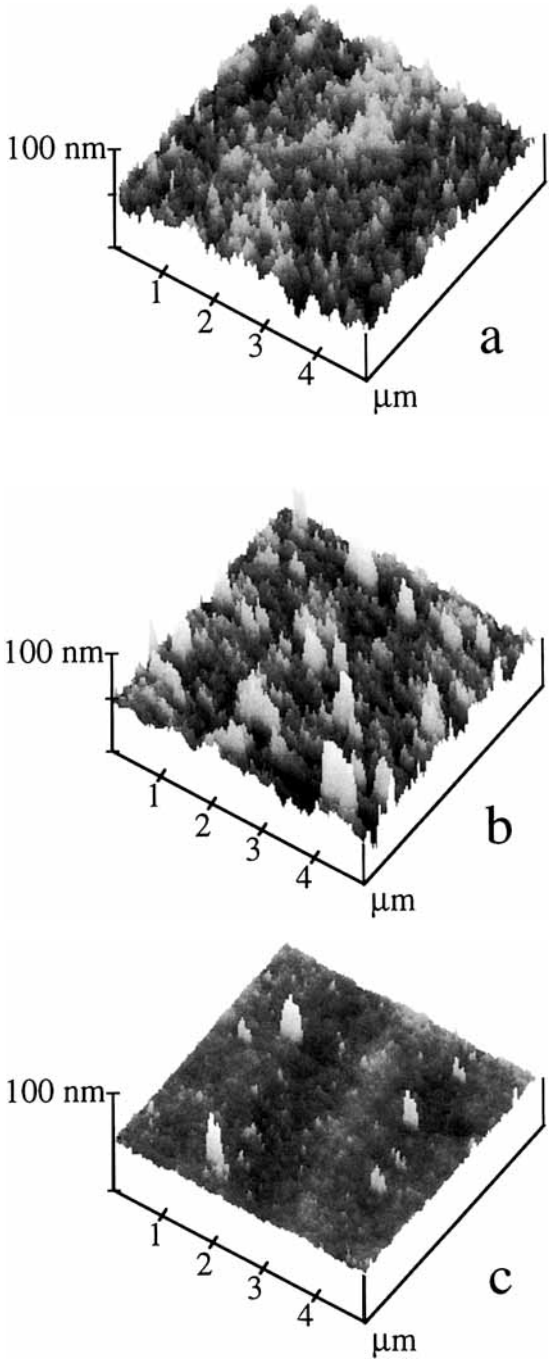

Figure 6 Atomic force micrographs of grafted Tecoflex films. The surface mean roughness (SMR) values were evaluated from corresponding micrographs with a surface area of 5 × 5 μm:

	a	b	c
Plasma treatment time (s)	10	300	300
Grafting density (μg PEG/cm^2)	91	340	517
Surface mean roughness (nm)	5.7	5.9	1.6

to note that a surface nitrogen content of 0% was observed for the grafted film with a very high PEG grafting density. If only judged from a total disappearance of N_{1S} peak on the surface, it seems reasonable to say that the grafted films with a very high PEG grafting density is completely covered with a PEG layer of a thickness of ca. 10 nm. The surface elemental composition of this grafted sample is, however, not exactly the same as that of pure PEGMA. A small insignificant difference of about 2% is detected both in carbon and oxygen content (Table III). It is already known that PTMG moieties tend to accumulate at the air-side surface of Tecoflex. Therefore, it may be reasonable to say that the grafted film with a very high PEG grafting density is completely covered by PEG with various thickness so that the XPS technique will detect a small fraction of PTMG moieties.

Atomic Force Microscopy

It is interesting to note that the surface topography of grafted films depends on both the PEG grafting density and the plasma treatment time. Plasma treatment makes the film rougher, but grafted PEG chains cause the film to be smoother again. The competitive result of these two opposite effects determines the surface topography of the grafted films. As can be seen by comparing Figure 4(b) with Figure 6(a), grafted PEG chains have little effect on the surface topography originating from plasma etching when the PEG grafting density is very low. But the effect of grafted PEG chains on smoothening the surface is clearly seen if grafting degree is high [Figs. 4(c) and 6(b)]. When the grafted film has a very high PEG grafting density, the roughness caused by plasma treatment is almost completely overshadowed by the grafted PEG layer and a very smooth surface almost comparable with that of the virgin film reoccurs [Figs. 4(c), 6(c), and 4(a)].

Contact Angle Measurement

Although all grafted films exhibit lower static contact angles than the virgin film (Table VII), it is not sufficient to prove graft copolymerization from contact angle data only because the film treated with argon plasma already has a fairly low contact angle. This was also observed for the graft copolymerization of acrylamide onto a polyethylene surface pretreated with a glow discharge.[24] However, the static contact angle of grafted films does decrease with grafting density, indicating a better water wettability for the grafted film with a higher PEG content. All grafted films also exhibit lower dynamic contact angles than the virgin film. The relationship between

Table VII Contact Angles for the Virgin Film, the Plasma-Treated Film, and the PEG Grafted Films

Sample	Grafting Density ($\mu g/cm^2$)	θs^a	θa^a	θr^a	$\theta a - \theta r^a$	θa^b	θr^b	$\theta a - \theta r^b$
Virgin film	/	58 ± 2.5	79 ± 1.3	44 ± 0.5	35	87 ± 1.6	47 ± 0.3	40
Plasma-treated film	/	38 ± 3.0	55 ± 2.0	15 ± 3.6	40	63 ± 3.8	14 ± 1.5	49
Grafted films	0.247	43 ± 3.6	61 ± 0.5	18 ± 0.2	43	66 ± 1.8	20 ± 1.3	44
	0.280	40 ± 2.2	58 ± 2.0	20 ± 0.4	38	62 ± 2.8	27 ± 0.2	35
	0.324	36 ± 1.8	55 ± 0.5	24 ± 0.2	31	59 ± 0.9	27 ± 0.1	32
	0.420	35 ± 0.9	53 ± 2.0	27 ± 0.4	26	55 ± 2.8	29 ± 0.1	26

The plasma treatment time is 300 sec. θs: static angle measured by captive bubble (air-water) method; θa and θr: average advancing and receding angle measured by Wilhelmy plate method for one sample with 4 cycles of measurement, respectively.

[a] Samples were hydrated in water for 2 days before measurement.

[b] Measurement was done on nonhydrated samples.

the dynamic contact angle and the grafting density, however, is not so simple as that between the static contact angle and grafting density. Contrary to what was originally expected, the receding angle of the grafted films increases with the grafting density, although the advancing angle decreases with grafting density. To understand this phenomenon, the contribution of plasma treatment to the reduction of the receding angle, even after graft copolymerization, should be taken into account. Because of roughness arising from surface etching and polar groups introduced by surface oxidation, the sample treated with 300-s argon plasma already had a surface with an extremely low receding contact angle (14 deg). The presence of grafted PEG chains on the surface smoothes the surface and overshadows part of the polar groups, which might be responsible for the increase in the receding angle. Nevertheless, the contact angle hysteresis ($\theta_a - \theta_r$) decreases with grafting density, indicating a smoother topography and probably a less composition-heterogeneous surface for the film with high PEG grafting density. This has already been proved directly by atomic force micrographs and indirectly by a higher surface PEG coverage from the XPS results.

Protein Adsorption

The adsorption of fibrinogen on the surface of hydrated grafted films was measured with an ELISA. As expected, lower fibrinogen adsorption was observed on grafted films with higher PEG grafting density (Table IV).

Immobilization of Heparin

In an attempt to verify the reactivity of the hydroxyl end groups that were built onto the surface of the Tecoflex film and to further improve the blood compatibility of Tecoflex, the immobilization of heparin was performed. As shown in Table VIII, the amount of heparin physically adsorbed on the nonactivated grafted film and the reference Tecoflex film is very low (less than 0.01 $\mu g/cm^2$), whereas about 1.1 $\mu g/cm^2$ of heparin was detected on the activated grafted film, demonstrating successful heparin immobilization.

CONCLUSION

Tecoflex films treated with argon plasma exhibited higher hydrophilicity and rougher topography than

Table VIII Amount of Heparin Physically Adsorbed and Immobilized on the Virgin and Grafted Tecoflex Films

Sample	Grafting Density (μg PEG/cm^2)	Buffer for Heparin Immobilization	Amount of Heparin ($\mu g/cm^2$)
Tecoflex	/	PBS (pH 7.4)	0.057
Nonactivated grafted film	120	PBS (pH 7.4)	0.057
Activated grafted film	120	PBS (pH 7.4)	1.08
		PBS (pH 9.0)	1.18

[a] PBS = phosphate-buffered solution.

virgin films. PEG chains were successfully grafted onto the surface of Tecoflex by PIGP of PEGMA. Grafted films with different surface grafting density of PEG as indicated by weight change and XPS results were prepared. The surface with high PEG grafting density exhibits smoother topography than the plasma-treated surfaces and grafted surfaces with low grafting density. The grafted films exhibit higher hydrophilicity than the virgin film as indicated by lower contact angles. Much lower fibrinogen adsorption on the surface of grafted films was observed by ELISA. The hydroxyl end groups on the surface offer further possibilities of improving its biocompatibility by immobilizing heparin.

Y. X. Qiu acknowledges the financial support of Alexander von Humboldt Foundation of Germany, the National Natural Science Foundation of China, and the State Commission of Science and Technology of China.

REFERENCES

1. M. D. Lelah and S. L. Cooper, *Polyurethane in Medicine*, CRC Press, Boca Raton, FL, 1986, pp. 57–110.
2. G. R. Llanos and M. V. Sefton, *J. Biomater. Sci., Polym. Ed.*, **4,** 381 (1993).
3. D. K. Han, K. D. Park, K. D. Ahn, S. Y. Jeong, and Y. H. Kim, *J. Biomed. Mater. Res.: Appl. Biomater.*, **23,** 87 (1989).
4. D. K. Han, S. Y. Jeong, and Y. H. Kim, *J. Biomed. Mater. Res.: Appl. Biomater.*, **23,** 211 (1989).
5. K. D. Park, T. Okano, C. Nojiri, and S. W. Kim, *J. Biomed. Mater. Res.*, **22,** 977 (1988).
6. K. D. Park, A. Z. Piao, H. Jacobs, T. Okano, and S. W. Kim, *J. Polym. Sci., Polym. Chem.*, **29,** 1725 (1991).
7. C. Freij-Larsson and B. Wesslen, *J. Appl. Polym. Sci.*, **50,** 345 (1993).
8. B. Wesslen, M. Kober, C. Freij-Larsson, A. Ljungh, and M. Paulsson, *Biomaterials*, **15,** 278 (1994).
9. Y. Ikada, *Biomaterials*, **15,** 725 (1994).
10. D. K. Han, S. Y. Jeong, Y. K. Kim, B. G. Min, and H. I. Cho, *J. Biomed. Mater. Res.*, **25,** 561 (1991).
11. D. K. Han, N. Y. Lee, K. D. Park, Y. H. Kim, H. I. Cho, and B. G. Min, *Biomaterials*, **16,** 467 (1995).
12. H. K. Yaduda, *J. Appl. Polym. Sci., Appl. Polym. Symp.*, **42,** 1988.
13. C. M. Chan, in *Polymer Surface Modification and Characterization*, Hanser Publishers, New York, 1993, Chap. 6.
14. K. Fujimoto, H. Inoue, and Y. Ikada, *J. Biomed. Mater. Res.*, **27,** 1559 (1993).
15. Y. H. Sun, W. R. Gombotz, and A. S. Hoffman, *J. Bioactive Compat. Polym.*, **1,** 316 (1986).
16. Y. H. Sun, A. S. Hoffman, and W. R. Gombotz, *ACS Polym. Prepr.*, **28,** 292 (1987).
17. K. Nilsson and K. Mosbach, *Biochem. Biophys. Res. Commun.*, **102,** 449 (1981).
18. J. M. Harris, E. C. Struck, M. G. Case, M. S. Paley, M. Yalpani, J. M. van Alstine, and D. E. Brooks, *J. Polym. Sci., Polym. Chem.*, **22,** 341 (1984).
19. P. K. Smith, A. K. Mallia, and G. T. Hermanson, *Anal. Biochem.*, **109,** 466 (1980).
20. T. Yasuda, T. Okuno, K. Yoshida, and H. Yasuda, *J. Polym. Sci., Polym. Phys. Ed.*, **26,** 1781 (1988).
21. M. Morra, E. Occhiello, R. Marola, F. Garbassi, P. Humphrey, and D. Johnson, *J. Colloid Interface Sci.*, **137,** 11 (1990).
22. H. C. van der Mei, I. Stokroos, J. M. Schakenraad, and H. J. Busscher, *J. Adhesion Sci. Technol.*, **5,** 757 (1991).
23. J. H. Chen and E. Ruckenstein, *J. Colloid Interface Sci.*, **135,** 496 (1990).
24. M. Suzuki, A. Kishida, H. Iwata, and Y. Ikada, *Macromolecules*, **19,** 1804 (1986).
25. M. E. Ryan and J. P. S. Badyal, *Macromolecules*, **28,** 1377 (1995).
26. M. Mori, Y. Uyama, and Y. Ikada, *J. Polym. Sci., Polym. Chem. Ed.*, **32,** 1683 (1994).
27. Y. M. Lee, S. Y. Ihm, J. K. Shim, J. H. Kim, C. S. Cho, and Y. K. Sung, *Polymer*, **36,** 81 (1995).
28. H. Ichijima, T. Okada, Y. Uyama, and Y. Ikada, *Makromol. Chem.*, **192,** 1213 (1991).
29. E. A. Kulik, K. Kato, M. I. Ivanchenko, and Y. Ikada, *Biomaterials*, **14,** 763 (1993).

Received February 7, 1996
Accepted April 8, 1996